

Transcription Inhibition Using Oligonucleotide-Modified Gold Nanoparticles

Chiamaka Agbasi-Porter, Jessica Ryman-Rasmussen,[†] Stefan Franzen,* and Daniel Feldheim*

Department of Chemistry, North Carolina State University, Raleigh, North Carolina 27695. Received April 21, 2006; Revised Manuscript Received June 16, 2006

The capture of T7 RNA polymerase using double-stranded promoter DNA on the surface of gold nanoparticles has been demonstrated. The competitive binding and inhibition of T7 RNA polymerase due to specific interactions on the nanoparticle surface represents a transcription factor decoy approach in a model system. The efficiency of inhibition was determined for various nanoparticle sizes, surface coverage, and linker length for double-stranded promoter DNA on gold nanoparticles. The experiments provide a basis for determining the accessibility of binding sites on nanoparticle surfaces for applications involving cell targeting or the use of nanoparticles as binding agents in solution.

INTRODUCTION

Methods for interrupting genetic transcription and translation have become invaluable in studying the molecular biology of cells and have shown promise as *in vivo* therapeutic reagents (1–10). Several strategies are available to manipulate gene expression at the DNA or RNA stages. By introducing whole genes into cells, gene therapy (2) works at the DNA level, effectively replacing aberrant mRNA with mRNA that codes for functional protein. In contrast, antisense oligonucleotides hybridize to mRNA to alter gene splicing or prevent translation (11–14). Yet another strategy for manipulating gene expression is to prevent transcription altogether by interfering with transcription factors (15–18). This can be accomplished by introducing a competitive binding agent into the cell, for example a DNA duplex sequence that mimics a transcription factor binding site on the gene of interest. The DNA duplex acts as a “decoy”, competitively binding to a transcription factor so that it is not available to perform its normal role in DNA transcription.

A critical limitation in the implementation of nearly all oligonucleotide therapeutic strategies remains the translocation of the active agent across cell and nuclear membranes. Oligonucleotides do not readily diffuse across cell membranes, and many transport vectors have been studied to aid in their cellular uptake. Nanoparticles with multiple targeting peptides have been observed to transit to both the cytoplasm and the nucleus of HepG2 and HeLa cell lines (19, 20). These observations of intracellular internalization of gold nanoparticles (5 nm to 20 nm in diameter) modified with cell and nuclear targeting peptides provides the impetus to study nucleotide interactions on nanoparticle surfaces. The present study focuses on the interaction of the dsDNA promoter sequence for T7 RNA polymerase (RNAP) attached to gold nanoparticles with RNAP in solution. We show that the promoter-modified particles can effectively compete with a template DNA sequence for RNAP. This study also addresses the ability of gold particles in the 5–15 nm size range to interact with a large protein.

EXPERIMENTAL PROCEDURES

Reagents. Citrate-coated gold nanoparticles (10 and 15 nm) were purchased from Ted Pella. NAP-10 columns were purchased from Pharmacia Biotech. *In vitro* transcription assay kit and RNAP were obtained from Promega. Freeze & Squeeze gel extraction kit, 40% Acrylamide/Bis solution 19:1, TEMED, and ammonium persulfate were purchased from Bio-Rad. Dithiothreitol (DTT) was obtained from Pierce Chem.

The oligonucleotide sequences used in this study are listed in Table 1. Oligonucleotides were purchased from MWG Biotech Inc or IDT. The bold sections of the oligonucleotide sequence indicate the promoter region for RNAP binding. The control strand was a sequence that lacks the promoter region for RNA polymerase.

Preparation of Decoy Oligonucleotide–Gold Conjugates. Thiolated oligonucleotides were received as disulfides. The disulfide was cleaved using a 100 mM solution of dithiothreitol (DTT) in 0.1 M sodium phosphate, pH 8.3 buffer. The reaction was allowed to proceed for 30 min at room temperature, after which the oligonucleotide was desalted and separated from DTT on a NAP-10 column. The purified solution of the DNA was quantified using the absorbance at 260 nm and the extinction coefficient for each specific sequence.

Decoy oligonucleotide–Au conjugates were prepared as described in the literature with few modifications (21). Briefly, 20 μ L or 7 μ L of a 200 μ M solution of the oligonucleotide were added to 500 μ L of 10 nm diameter or 15 nm diameter colloidal gold solution, respectively. The final concentrations of decoy oligonucleotide and gold particles were 8 μ M and 9.5 nM for 10 nm diameter particles, and 3 μ M and 2.3 nM for 15 nm diameter particles, respectively. The samples were placed in a water bath at 37 °C for 4 h, after which the solution was diluted with 0.1 M NaCl/10 mM Na phosphate pH 7 to a total volume of 800 μ L. The samples were incubated in the solution for at least 16 h at 37 °C. Following this, samples were centrifuged at 14 000g for 30 min and rinsed with 500 μ L of 0.1 M NaCl/10 mM Na phosphate. After this procedure was repeated three times, the samples were resuspended in 0.3 M NaCl/10 mM Na phosphate to a final volume of 200 μ L.

Mixed monolayers of decoy oligonucleotide/mercaptohexanol (MCH) were prepared by simultaneous addition of decoy oligonucleotide and MCH to gold nanoparticles. This was accomplished by adding 60 μ L of 200 μ M oligonucleotide solution, and 2.5 μ L or 1 μ L of 500 μ M MCH to 2.5 mL of 10

* Address correspondence to Stefan_Franzen@NCSU.edu and Dan_Feldheim@NCSU.edu.

[†] Current address: Center for Chemical Toxicology Research and Pharmacokinetics, College of Veterinary Medicine, North Carolina State University, Raleigh, NC 27695.

Table 1. Sequences of Modified Double-Stranded Oligonucleotides Used in This Work

name	sequence
template	HS-(CH ₂) ₆ -TAATACGACTCACTATAGGGGGATCGAAGTTAGTAGGCCCC ATTATGCTGAGTGATATCCCCCTAGCTTCAATCATCCGGG
decoy	HS-(CH ₂) ₆ -5'-TAATACGACTCACTATAGGGG-3' 3'-ATTATGCTGAGTGATATCCCC-5'
Rd-DNA	5'-ATTATGCTGAGTGATATCCCC-3'-rhodamine
control	HS-(CH ₂) ₆ -5'-AACCAGGATTATCCGCTCAC-3' 3'-TTGGTCCTAATAGGCGAGTG-3'

Table 2. Number of Single-Stranded Oligonucleotides per Nanoparticle

linker ^a	10 nm diameter particles: mole fraction of ssDNA during preparation			15 nm diameter particles: mole fraction of ssDNA during preparation		
	1	0.9	0.75	1	0.9	0.75
C ₆	148 ± 2	131 ± 2	122 ± 5	220 ± 6	207 ± 4	194 ± 2
C ₆ -A ₆	133 ± 1	127 ± 4	112 ± 2	214 ± 2	197 ± 5	188 ± 1
C ₆ -EG ₃	124 ± 2	117 ± 6	105 ± 3	204 ± 5	190 ± 4	184 ± 2
C ₆ -EG ₆	111 ± 3	93 ± 5	81 ± 1	180 ± 1	175 ± 3	167 ± 2

^a C₆ denotes six methylene units in the linker, A₆ denotes six adenine units, and EG_n denotes the number of ethylene glycol units.

Table 3. Number of Double-Stranded Oligonucleotides per Nanoparticle

linker	10 nm diameter particles: mole fraction of ssDNA during preparation			15 nm diameter particles: mole fraction of ssDNA during preparation		
	1	0.9	0.75	1	0.9	0.75
C ₆	39 ± 6	47 ± 5	50 ± 7	94 ± 2	100 ± 4	130 ± 3
C ₆ -A ₆	54 ± 3	60 ± 5	75 ± 2	122 ± 1	138 ± 2	151 ± 3
C ₆ -EG ₃	61 ± 5	77 ± 4	98 ± 2	142 ± 5	155 ± 2	179 ± 3
C ₆ -EG ₆	38 ± 7	46 ± 3	62 ± 1	132 ± 3	143 ± 2	159 ± 5

Table 4. Percentage of ssDNA per Particle That Hybridized To Form dsDNA

linker	10 nm diameter particles: mole fraction of ssDNA during preparation			15 nm diameter particles: mole fraction of ssDNA during preparation		
	1	0.9	0.75	1	0.9	0.75
C ₆	26%	36%	41%	43%	48%	67%
C ₆ -A ₆	40%	47%	67%	57%	70%	80%
C ₆ -EG ₃	49%	66%	93%	70%	82%	97%
C ₆ -EG ₆	34%	49%	77%	73%	82%	95%

nm diameter or 5 mL of 15 nm diameter gold nanoparticles, respectively, and allowing the reaction to proceed for 8 h. The reaction mixture was subsequently diluted with 0.1 M NaCl/10 mM Na phosphate pH 7 to a total volume of 4 mL and 9.5 mL for 10 and 15 nm gold nanoparticles, respectively. The samples were incubated in the solution for at least 16 h. The resulting nanoparticles were centrifuged three times at 14 000g for 30 min and washed with 500 μ L of 0.1 M NaCl/10 mM Na phosphate between centrifugations. The samples were resuspended in 0.3 M NaCl/10 mM Na phosphate to a final volume of 1.5 mL.

To quantify surface-bound oligonucleotides, the nanoparticles were oxidatively etched with 0.1 M KCN. The freed oligonucleotides in solution were then quantified using OliGreen ssDNA Quantitation Kit (Molecular Probes) according to manufacturer's directions. The fluorescence was analyzed by a BioTek FL-600 plate reader.

To determine the number of oligonucleotides hybridized per nanoparticle, fluorophore-labeled oligonucleotides, which were complementary to the surface-bound oligonucleotides, were allowed to hybridize to the gold nanoparticles. Oligonucleotide-gold conjugates were prepared as described above and resuspended into a final volume of 300 μ L of 0.1 M NaCl/10 mM sodium phosphate at pH 7.0. 20 μ L of 100 μ M fluorophore-labeled complement was added to the decoy oligonucleotide-gold conjugates. The samples were heated to 35 °C for 1 h and then allowed to anneal while cooling to room-temperature overnight in a water bath. After hybridization, the conjugates were centrifuged three times at 14 000 rpm for 30 min, washing

with 200 μ L of 0.3 M NaCl/10 mM sodium phosphate pH 7 buffer between centrifugations. Conjugates were resuspended into a final volume of 200 μ L. The fluorophore-labeled oligonucleotides were denatured by addition of NaOH (final concentrated ~50 mM, pH 11). After 2 h, the conjugates were centrifuged again at 14 000 rpm for 30 min. The pH of the supernatant was adjusted to 9 with 1.0 M HCl, and the fluorescence was analyzed by a BioTek FL-600 plate reader.

Transcription Assay. A competitive in vitro runoff transcription assay was performed utilizing a modification of the manufacturer's (Promega) instructions. Five micrograms (194 pmol) of the T7 DNA template was mixed with 80 units of RNAP, 33.3 mM nucleotide triphosphates (NTPs), and increasing concentrations of 10 and 15 nm decoy modified gold nanoparticles in a final reaction volume of 100 μ L. The reaction was allowed to proceed for 16 h at 37 °C. The reaction mixture was spun at 14 000g for 30 min to pellet the gold nanoparticles, and 10 μ L of the supernatants was run on a native 6% polyacrylamide gel in glycine-HCl buffer at 100 V for 90 min. The mRNA product was revealed by staining the gel with 0.45 μ g/mL ethidium bromide. mRNA bands were excised, and the RNA was extracted with the Freeze & Squeeze Gel Extraction kit (Bio-Rad) according to instructions. The mRNA content of the excised bands was quantified by measuring the absorbance at 260 nm in a Hewlett-Packard 8453 Chemstation photodiode array spectrophotometer. All transcriptions were done in triplicate.

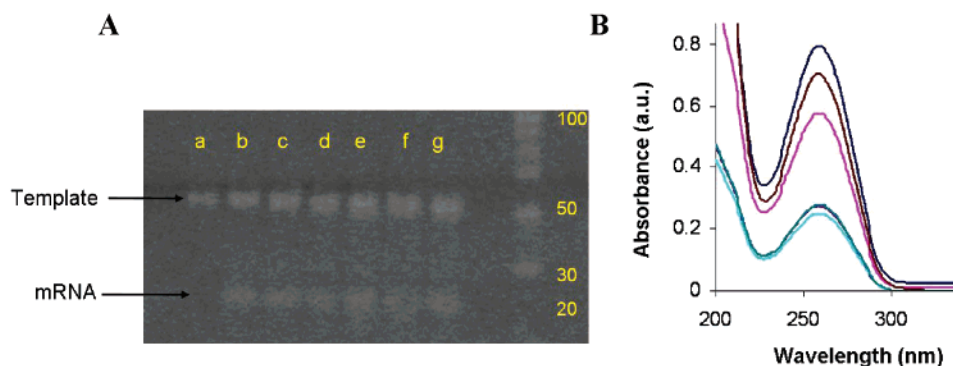


Figure 1. (A) 6% PAGE gel of transcripts after transcription assay. Lanes a) DNA template, b) no gold nanoparticles, c–g) 0.80 nM, 2.3 nM, 7.8 nM, and 11 nM, respectively, of 10 nm gold nanoparticles at 39 decoys/particle. (B) UV–visible spectra of mRNA following gel purification. Spectra correspond to material extracted from lanes b to g going from highest to lowest absorbance peak.

RESULTS

The effects of decoy surface density on RNAP binding were first studied by assembling mixed monolayers of the hexanethiol-terminated ssDNA decoy sequence (HS-(CH₂)₆-Decoy) and mercaptohexanol (MCH) on gold nanoparticles and then hybridizing the complement to form the fully double-stranded decoy sequence. Within the mole fractions studied (solution oligonucleotide mole fractions of 0.9, 0.75, and pure DNA), it was found that lowering the surface density of ssDNA increased the yield of duplex formation on the particle surface for both 10 and 15 nm diameter gold nanoparticles (Tables 2–4). A maximum of 50 ± 7 and 130 ± 3 duplexes per particle was found for 10 and 15 nm diameter particles, respectively, using a mole fraction of 0.75. Smaller mole fractions of DNA were investigated; however, particle aggregation was observed during preparation.

A transcription competition assay was used to compare *in vitro* inhibition of transcription by gold nanoparticles carrying the T7 transcription factor decoy as a function of particle diameter and number of dsDNA transcription factor decoys per particle. In a typical assay, the dsDNA template was incubated in solution with increasing concentrations of 10 or 15 nm diameter decoy-capped gold nanoparticles in the presence of NTPs and RNAP. After the transcription reaction was completed, the reaction mixture was centrifuged to separate the nanoparticles from the template and mRNA transcript (supernatants). The supernatants were eluted on a 6% PAGE gel, and the transcript bands were removed and purified by freeze and squeeze extraction. Figure 1A shows a representative PAGE gel. Lane a in Figure 1A is a sample containing only the dsDNA template, while lane b contains the template that had been transcribed with T7 polymerase in the absence of nanoparticles carrying the decoy. Lanes c–g are samples in which the transcription was performed in the presence of increasing concentrations of 10 nm diameter gold nanoparticles modified with 39 ± 6 decoy oligonucleotides per particle. The top band in each lane corresponds to the dsDNA template, and the second band contains mRNA transcript. To quantify the amount of mRNA produced in each transcription, the second band from each lane was excised, and the mRNA was purified and analyzed by UV–visible spectroscopy.

The spectra presented in Figure 1B show that the T7 promoter-modified nanoparticles inhibited transcription of the template DNA. At the highest nanoparticle concentration, transcription was inhibited by approximately 80%. To determine if the inhibition of mRNA observed during the transcription assay was due to the oligonucleotide-capped gold nanoparticle decoy, controls were performed in which unmodified nanoparticles and nanoparticles modified with duplex DNA lacking the T7 promoter region were added to the transcription assay.

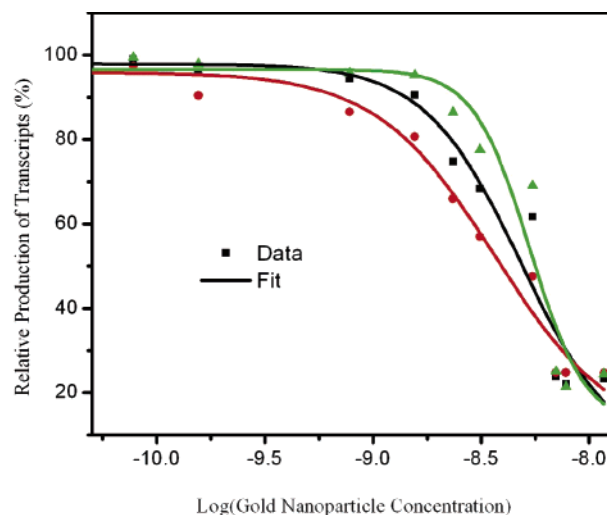


Figure 2. Dose–response curves used in the determination of IC₅₀ values for decoy-modified 10 nm gold nanoparticles. The curves are (black) 1.2×10^{13} decoy/cm², (green) 1.5×10^{13} decoy/cm², (red) 1.6×10^{13} dsDNA decoy was bound to particles via a hexanethiol linker.

Transcription of the template was not inhibited in either experiment. This suggests that the oligonucleotide-capped gold nanoparticle decoy does play a specific role in the down regulation of RNA transcription by RNAP. It was then of interest to quantitatively assess transcription inhibition by nanoparticles of different sizes and decoy coverages.

To make quantitative comparisons between different nanoparticle decoys, the IC₅₀ was determined. The IC₅₀, or 50% inhibition concentration values, were determined by plotting relative production of mRNA vs log nanoparticle concentration (dose–response curves, Figure 2). The dose–response curves showed, for a given particle size, only a modest change in IC₅₀ as a function of decoy density (Table 5). The lowest density particles displayed an approximately 50% greater inhibition than the particles that were fully covered with the T7 promoter sequence. A much more important parameter appears to be particle size. Increasing particle size from 10 to 15 nm in diameter decreased IC₅₀ by a factor of roughly 5 (Table 5). This is not solely a surface area effect since the surface area of 15 nm diameter particles is only a factor of 2 larger than that of 10 nm particles.

Another potential method for minimizing the effects of sterics on T7 polymerase binding to decoy-modified nanoparticles is to add a longer spacer between the promoter sequence and the particle surface. Three spacers were chosen to test this hypothesis, HS-(CH₂)₆-Adenine₆-Decoy (C₆-A₆), HS-(CH₂)₆-[OCH₂-CH₂O]₃-Decoy (C₆-EG₃), and HS-(CH₂)₆-[OCH₂CH₂O]₆-Decoy

Table 5. Coverages and IC₅₀ Values of Oligonucleotide-Capped Gold Nanoparticles with Different Linkers

mole fraction of ssDNA during preparation	dsDecoys/cm ² (10 nm dia.) × 10 ¹³	IC ₅₀ , 10 nm dia. (nM)	dsDecoys/cm ² (15 nm dia.) × 10 ¹³	IC ₅₀ , 15 nm dia. (nM)
		C₆		
1	1.2 ± 0.1	5.3 ± 0.9	1.3 ± 0.1	1.4 ± 0.6
0.9	1.5 ± 0.2	4.8 ± 0.7	1.5 ± 0.1	0.93 ± 0.4
0.75	1.6 ± 0.2	3.2 ± 0.4	1.8 ± 0.1	0.85 ± 0.4
		C₆-A₆		
1	1.7 ± 0.1	5.1 ± 0.2	1.7 ± 0.1	0.94 ± 0.2
0.9	1.9 ± 0.2	4.6 ± 0.8	2.0 ± 0.1	0.89 ± 0.1
0.75	2.4 ± 0.1	3.8 ± 0.6	2.1 ± 0.1	0.85 ± 0.5
		C₆-EG₃		
1	1.9 ± 0.1	4.8 ± 0.5	2.0 ± 0.1	0.90 ± 0.3
0.9	2.4 ± 0.1	4.1 ± 0.8	2.2 ± 0.1	0.85 ± 0.2
0.75	3.1 ± 0.2	3.5 ± 0.6	2.5 ± 0.1	0.79 ± 0.4
		C₆-EG₆		
1	1.2 ± 0.1	4.3 ± 0.8	1.9 ± 0.1	0.85 ± 0.5
0.9	1.5 ± 0.1	3.7 ± 0.9	2.0 ± 0.1	0.81 ± 0.3
0.75	2.0 ± 0.1	3.3 ± 0.4	2.2 ± 0.1	0.72 ± 0.2

(C₆-EG₆). Again, it was found that lowering the surface density of ssDNA increased the yield of duplex formation on the particle surface (Tables 3 and 4). A maximum of 77 ± 4 and 155 ± 2 duplexes per particle were found for 10 and 15 nm diameter particles, respectively, for the C₆-EG₃ linker at a mole fraction of 0.75. Surprisingly, the longer chain, C₆-EG₆, yielded less total hybridized dsDNA per particle than the shorter linkers, and a lower or comparable percentage of hybridized DNA than all but the C₆ linker. A comparison of IC₅₀ values between linkers at constant particle size and mole fraction revealed a slight decrease in IC₅₀ with increasing linker length in all but two cases. It is noteworthy that despite the relatively low coverage of dsDNA for particles modified with C₆-EG₆ (Table 3), IC₅₀ values were lowest for this linker (Table 5).

DISCUSSION

The present study addresses the effects of steric crowding on the ability of proteins to recognize DNA-modified gold nanoparticles. One advantage of using gold nanoparticles in biological assays is that cooperative effects may enhance the binding of target molecules with biomolecules attached to the particles surface. This has been shown to improve internalization efficiencies of nanoparticles into cells (19–22) and greatly improve DNA hybridization assays (23, 24). Indeed, dsDNA has been reported to be more stable when hybridized on the surface of a gold nanoparticle, yielding binding constants that are enhanced by two orders-of-magnitude compared to the identical sequences hybridized in solution (25). However, when a larger biomolecule such as T7 polymerase interacts with a dsDNA promoter sequence attached to a gold nanoparticle, one might expect that steric hindrance could negate any advantage afforded by the high density of DNA decoy strands on the nanoparticle. Thus, our main objective was to assess the role of steric interactions in a nanoparticle-based transcription factor decoy approach.

The role of oligonucleotides conjugated to nanoparticle surfaces in promoting nanoparticle interactions with proteins and complementary oligonucleotides has been probed in the present experiments using both differing surface concentrations of oligonucleotides and tether lengths. The congestion at the surface of a colloidal gold particle could affect the binding of proteins and the ability of DNA or RNA to hybridize. Such congestion will have functional consequences for cell targeting experiments. For this reason it is of interest to understand whether nanoparticles prepared with a high concentration of surface-bound species are able to interact with biological macromolecules.

The yield of DNA hybridization for three different surface concentrations of ssDNA was considered first. The surface

concentration of ssDNA was diluted by mercaptohexanol (MCH), a passivating molecule that competes effectively with thiol-labeled ssDNA molecules for the gold surface. The importance of dilution in permitting sufficient freedom of the surface-attached ssDNA chains for hybridization was clearly demonstrated on both 10 and 15 nm particles. The implication from Tables 2–4 is that the hybridization increases as the surface density of oligonucleotides decreases. Similar observations have been made on gold nanoparticles, where hybridization efficiencies approaching 98% were also reported (21), and on planar gold surfaces where the maximum hybridization efficiency was observed for approximately 40% coverage by ssDNA (26). We would expect that the maximum hybridization yield would occur when the ssDNA chains are behaving as free nonentangled Gaussian chains. For Gaussian chain behavior the average diameter of the ssDNA would be $d = L\sqrt{N}$, where L is the distance between each successive monomer and N is the number of monomers. For ssDNA there are six single bonds separating each base (C5'-O-P-O-C3'-C4'-C5'). For the 21-mer sequence with a C₆ spacer (six carbon spacer) used in the transcription factor decoy experiments there are $N = 6 \times 22 = 132$ bonds (including the spacer) with an average bond length of $L = 1.55$ Å, we can estimate the Gaussian chain length to be $d = 1.8$ nm. We assume that the projection of the Gaussian chain length d on the surface gives the radius of gyration $r = d \cos \theta$. This simple model neglects the radius of curvature of the gold nanoparticle surface. Given this value, the area swept out by a tethered rotating ssDNA on the surface is approximately $\pi d^2 \cos^2 \theta = 4.2$ nm², if the projection angle θ on the surface is 50° as shown in Figure 3. The surface area of 10 and 15 nm nanoparticles are 314 nm² and 707 nm², respectively. Dividing the total surface area by the surface projection per free rotating ssDNA monomer gives an estimated maximum surface coverage of 74 and 168 ssDNA for 10 and 15 nm gold particles, respectively. If we assume that the requirement for efficient hybridization is that the ssDNA chains are free to rotate so that they can adopt a full range of conformations, and then maximum dsDNA coverage should correspond approximately to these values. These numbers compare reasonably well to the maximum values of 75 and 150 given in Table 2. If the ssDNA concentration is higher, then there is entanglement and restriction of motion leading to reduced hybridization yield.

The effect of spacer length can be to increase the freedom of the chains; however, this effect competes with an increase in the radius of gyration on the surface. The C₆-EG₃ and C₆-EG₆ chains have an increase of 9 and 18 bonds, respectively, compared to C₆. These linkers increase the Gaussian chain length by approximately 0.5 nm per EG₃ unit (i.e. 0.5 nm for EG₃ and 1.0 nm for EG₆). The longer chain and higher radius of gyration

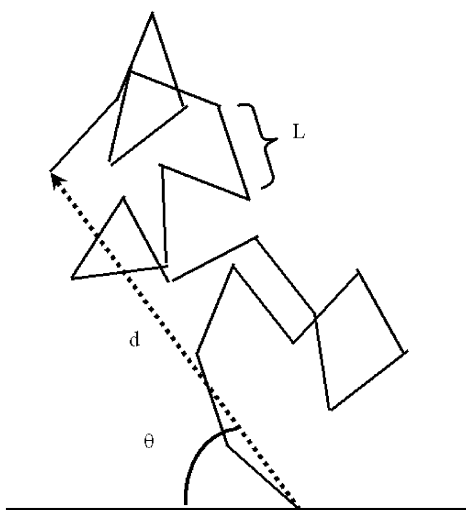


Figure 3. Illustration of the Gaussian chain length model for surface-attached oligonucleotides. The bond length is L . The angle of vector d with respect to the surface is θ .

tends to decrease the surface coverage at which maximum free rotation occurs (if the angle remains the same). For example, this model predicts that the coverage will decrease from 75 (C_6) to 67 (C_6 -EG₆) for 10 nm particles and from 168 (C_6) to 151 (C_6 -EG₆) for 15 nm particles due to the longer Gaussian chain length. To quantitatively explain the coverages given in Table 2 using the tethered Gaussian chain in Figure 3. Specifically, if the angle θ increases to 55° for the C_6 -EG₃ linker, the predicted optimal surface coverage is 90 and 200 ssDNAs on 10 and 15 nm gold nanoparticles, respectively, which is in reasonable agreement with the data in Tables 2-4.

The binding of RNAP to the transcription factor decoy on the surface was probed by determining the IC₅₀ value for inhibition of transcription in solution. The ability of RNAP to bind to dsDNA on nanoparticles with high surface densities is clearly hindered when compared to the binding to the same sequence in solution. The IC₅₀ value for transcription inhibition using free decoy was found to be 1.1 pM. However, given its molar mass of 98 kDa, the fact that RNAP binds to decoy modified nanoparticles to the extent observed in this study indicates that there is a some free volume in these bioconjugates. Despite the lower surface coverage measured for decoys bound to nanoparticles through the C_6 -EG₆ linker, this linker provided the optimum chain length for transcription inhibition. The results presented here thus serve to illustrate the importance of sterics in the design of nanoparticle bioconjugates for protein recognition. Short linkers or densely packed ssDNA monolayers can hinder both dsDNA formation and protein binding. The coverage of dsDNA, on the other hand, is actually highest for the C_6 -EG₃ linker and decreases slightly for the longer the C_6 -EG₆ linker. This effect may be due to greater entanglement of the complementary ssDNA strand if the nanoparticle-surface-bound ssDNA strand has many degrees of freedom.

One result from the current work appears to be that there is a confinement effect that hinders surface binding on small nanoparticles. We can use the transcription factor decoy assay to compare the functional binding of RNAP to oligonucleotides in solution and on nanoparticle surfaces. The binding of RNAP to oligonucleotides free in solution is ~2.5 orders-of-magnitude more favorable than binding to the same oligonucleotide on a 15 nm nanoparticle. The binding of RNAP to a tethered oligonucleotide (as represented by the IC₅₀ value) is a factor of 5 stronger on a 15 nm nanoparticle than on a 10 nm nanoparticle that has the same coverage in terms of oligonucleotides/cm². This result is somewhat surprising since the radius of curvature

is larger for the small particle, and this may be interpreted as providing greater access to the surface-attached promoter sequence for RNAP. This effect is counterbalanced by the avidity of the larger nanoparticle. On a per nanoparticle basis, a 15 nm particle has roughly twice the number of binding sites per particle.

CONCLUSIONS

The availability of surface-attached ssDNA and dsDNA on the surface of nanoparticles for binding has been probed both in terms of surface density and chain length of the linker between the oligonucleotide and the gold surface. The key results are that the optimum surface coverage for ssDNA requires a mole fraction of 0.25 for a relatively short surface passivation molecule such as MCH, and that the optimum chain length for both DNA hybridization and RNAP binding includes an EG₃ spacer adding nine bonds to the linker and greater conformational freedom of ether (CH₂OCH₂) bonding compared to aliphatic (CH₂CH₂CH₂) bonding. However, the enhancement of DNA hybridization promoted by the EG₃ spacer is a modest effect overall of ~10% on 15 nm particles and at most 60% on 10 nm particles. The inhibition of transcription has been demonstrated and while the binding of T7 to a surface-attached promoter sequence is clearly reduced significantly compared to a free oligonucleotide, the ability of nanoparticles to interact with DNA-binding proteins has been quantitatively demonstrated.

ACKNOWLEDGMENT

This work was supported by NIH grant CA098194.

LITERATURE CITED

- Jia, F. Y., Shimomura, T., Niyibizi, C., and Woo, S. L. Y. (2005) Downregulation of human type III collagen gene expression by antisense oligodeoxynucleotide. *Tissue Eng.* 11, 1429–1435.
- Yamanaka, K., Rocchi, P., Miyake, H., Fazli, L., Vessella, B., Zangemeister-Witke, U., and Gleave, M. E. (2005) A novel antisense oligonucleotide inhibiting several antiapoptotic Bcl-2 family members induces apoptosis and enhances chemosensitivity in androgen-independent human prostate cancer PC3 cells. *Mol. Cancer Ther.* 4, 1689–1698.
- Tai, C. K., Wang, W. J., Logg, C. R., Solly, S., Frisen, C., Eiden, M. V., Klatzmann, D., Chen, T. C., and Kasahara, N. (2004) Replicative viral vectors for cancer: Quo vadis? *Cancer Gene Ther.* 11, 853–853.
- Correnti, J. M. and Pearce, E. J. (2004) Transgene expression in *Schistosoma mansoni*: introduction of RNA into schistosomula by electroporation. *Mol. Biochem. Parasitol.* 137, 75–79.
- Krull, C. (2004) Manipulating gene expression in chick. *FASEB J.* 18, A762-A763.
- Higashi, K., Inagaki, Y., Fujimori, K., Nakao, A., Kaneko, H., and Nakatsuka, I. (2003) Interferon-gamma interferes with transforming growth factor-beta signaling through direct interaction of YB-1 with Smad3. *J. Biol. Chem.* 278, 43470–43479.
- Segal, G., Song, R. T., and Messing, J. (2003) A new opaque variant of maize by a single dominant RNA-interference-inducing transgene. *Genetics* 165, 387–397.
- Stier, S., Cheng, T., Forkert, R., Lutz, C., Dombrowski, D. M., Zhang, J. L., and Scadden, D. T. (2003) Ex vivo targeting of p21-(Cip1/Waf1) permits relative expansion of human hematopoietic stem cells. *Blood* 102, 1260–1266.
- Beeri, R., Guerrero, J. L., Supple, G., Sullivan, S., Levine, R. A., and Hajjar, R. J. (2002) New efficient catheter-based system for myocardial gene delivery. *Circulation* 106, 1756–1759.
- Lessard, P. A., Kulaveerasingam, H., York, G. M., Strong, A., and Sinskey, A. J. (2002) Manipulating gene expression for the metabolic engineering of plants. *Metab. Eng.* 4, 67–79.
- Sierakowska, H., Sambade, M. J., Agrawal, S., and Kole, R. (1996) Repair of thalassemic human beta-globin mRNA in mammalian cells

- by antisense oligonucleotides. *Proc. Natl. Acad. Sci. U.S.A.* 93, 12840–12844.
- (12) Sazani, P., Gemignai, F., Kang, S. H., Maier, M., Manoharan, M., Persmark, M., Bortner, D., and Kole, R. (2002) Systemically delivered antisense oligomers upregulate gene expression in mouse tissues. *Nat. Biotechnol.* 20, 1228–1233.
- (13) Tomita, N. and Morishita, R. (2004) Antisense oligonucleotides as a powerful molecular strategy for gene therapy in cardiovascular diseases. *Curr. Pharm. Des.* 10, 797–803.
- (14) Cho-Chung, Y. S. (2000) Antisense and therapeutic oligonucleotides: toward a gene-targeting cancer clinic. *Expert Opin. Ther. Pat.* 10, 1711–1724.
- (15) Xi, S. C., Gooding, W. E., and Grandis, J. R. (2005) In vivo antitumor efficacy of STAT3 blockade using a transcription factor decoy approach: implications for cancer therapy. *Oncogene* 24, 970–979.
- (16) Martin, J. I., Broaddus, W. C., and Fillmore, H. I. (2004) A transcription factor decoy oligonucleotide that mimics the MMP-1 functional single nuclear polymorphism: A novel therapeutic for the inhibition of MMP-1 expression. *Neuro-Oncology* 6, 333–333.
- (17) Ahn, J. D., Kim, C. H., Magae, J., Kim, Y. H., Kim, H. J., Park, K. K., Hong, S. H., Park, K. G., Lee, I. K., and Chang, Y. C. (2003) E2F decoy oligodeoxynucleotides effectively inhibit growth of human tumor cells. *Biochem. Biophys. Res. Commun.* 310, 1048–1053.
- (18) Mann, M. J. and Dzau, V. J. (2000) Therapeutic applications of transcription factor decoy oligonucleotides. *J. Clin. Invest.* 106, 1071–1075.
- (19) Tkachenko, A. G., Xie, H., Coleman, D., Glomm, W., Ryan, J., Anderson, M. F., Franzen, S., and Feldheim, D. L. (2003) Multifunctional gold nanoparticle-peptide complexes for nuclear targeting. *J. Am. Chem. Soc.* 125, 4700–4701.
- (20) Tkachenko, A. G., Xie, H., Liu, Y. L., Coleman, D., Ryan, J., Glomm, W. R., Shipton, M. K., Franzen, S., and Feldheim, D. L. (2004) Cellular trajectories of peptide-modified gold particle complexes: Comparison of nuclear localization signals and peptide transduction domains. *Bioconjugate Chem.* 15, 482–490.
- (21) Pena, S. R. N., Raina, S., Goodrich, G. P., Fedoroff, N. V., and Keating, C. D. (2002) Hybridization and enzymatic extension of Au nanoparticle-bound oligonucleotides. *J. Am. Chem. Soc.* 124, 7314–7323.
- (22) Xie, H., Tkachenko, A. G., Glomm, W. R., Ryan, J. A., Brennaman, M. K., Papanikolas, J. M., Franzen, S., and Feldheim, D. L. (2003) Critical flocculation concentrations, binding isotherms, and ligand exchange properties of peptide-modified gold nanoparticles studied by UV–visible, fluorescence, and time-correlated single photon counting spectroscopies. *Anal. Chem.* 75, 5797–5805.
- (23) Storhoff, J. J., Elghanian, R., Mucic, R. C., Mirkin, C. A., and Letsinger, R. L. (1998) One-pot colorimetric differentiation of polynucleotides with single base imperfections using gold nanoparticle probes. *J. Am. Chem. Soc.* 120, 1959–1964.
- (24) Cao, Y. C., Jin, R. C., Thaxton, S., and Mirkin, C. A. (2005) A two-color-change, nanoparticle-based method for DNA detection. *Talanta* 67, 449–455.
- (25) Lytton-Jean, A. K. R., and Mirkin, C. A. (2005) A thermodynamic investigation into the binding properties of DNA functionalized gold nanoparticle probes and molecular fluorophore probes. *J. Am. Chem. Soc.* 127, 12754–12755.
- (26) Steel, A. B., Herne, T. M., and Tarlov M. J. (1998) Electrochemical quantitation of DNA immobilized on gold. *Anal. Chem.* 70, 4670–4677.

BC060100F